



ELSEVIER

International Journal of Solids and Structures 41 (2004) 3395–3410

INTERNATIONAL JOURNAL OF
SOLIDS and
STRUCTURES

www.elsevier.com/locate/ijsolstr

Solution to line loading of a semi-infinite solid in gradient elasticity

S. Li, I. Miskioglu ^{*}, B.S. Altan

ME-EM Department, Michigan Technological University, 1400 Townsend Dr., Houghton, MI 49931, USA

Received 28 January 2004; received in revised form 28 January 2004
Available online 12 March 2004

Abstract

A semi-infinite elastic solid subjected to line loading is considered with higher order boundary conditions is utilized to obtain a general solution in terms of Fourier integral transforms for a symmetrical line loading with prescribed normal tractions. The boundary conditions are obtained by variational method and shown that they differ from the boundary conditions reported in the literature for the simple theory. Closed form solutions are then obtained for a concentrated normal force (the Flamant problem), for constant normal traction, and a typical Hertzian normal traction distribution from classical elasticity. It is verified that undesirable displacement singularity predicted by classical elasticity in the Flamant problem is eliminated by the gradient elasticity solution. The solution for constant normal tractions also illustrate the capability of gradient elasticity to predict size effect by taking into account the effect of micro-structure, which classical elasticity does not adequately describe.

© 2004 Elsevier Ltd. All rights reserved.

Keywords: Line loading; Gradient elasticity; Fourier integral transforms; Variational method; Flamant problem; Size effect

1. Introduction

For linear elastic materials with micro-structure, Mindlin's generalized elasticity theory (Mindlin, 1964, 1965) provides a general framework for developing strain-gradient theories. Mindlin's generalized elasticity theory has been widely used to revisit problems where classical elasticity yields physically undesirable results. For example, Vardoulakis and Georgiadis (1997) have shown the existence of SH surface waves in a homogeneous half-space within the framework of the generalized linear theory of elasticity, which cannot be predicted by the classical theory of linear elasticity. They also investigated the anti-plane shear Lamb's problem (Georgiadis and Vardoulakis, 1998). Zhang et al. (1998) used the couple stress theory (Toupin, 1962; Koiter, 1964; Mindlin, 1964, 1965) to obtain the mode III full-field solution in elastic materials with strain gradient effects, and they showed that their evaluation results in a finite crack tip energy release rate which when evaluated by classical theory leads to an infinite value. Altan and Aifantis (1992) used a simple

^{*} Corresponding author. Tel.: +1-906-4872752; fax: +1-906-4872822 (I. Miskioglu).

E-mail address: imiski@mtu.edu (I. Miskioglu).

gradient theory of elasticity to solve the mode-III crack problem and found that the gradient theory can eliminate the undesirable singularity at the crack tip. Aifantis (1996) has shown that the gradient theory can successfully be used to interpret size effects exhibited by elastic boreholes and twisted wires. Within the context of the simple gradient theory of elasticity, Gutkin (2000) described the elastic property of dislocation and disclinations. The main achievement made in this approach is the elimination of the classical singularities at the defect line and the possibility of describing short-range interactions between defects on a nanoscale level.

The modification of the constitutive equation proposed by Mindlin (1965) within the framework of gradient elasticity reads

$$\sigma = \lambda(\mathbf{I} - c_1\mathbf{I}\nabla^2 - c_2\nabla\nabla)(\text{tr } \epsilon) + 2G(1 - c_3\nabla^2)\epsilon, \quad (1)$$

where λ and G are the Lame's constants, σ and ϵ denote elastic stress and strain tensors, respectively, \mathbf{I} is the unit tensor, ∇^2 is the Laplacian operator, and c_1 , c_2 and c_3 are three independent material constants.

The above formulation involves five elastic constants, and application of it to practical situations poses difficulties. A simplification to Eq. (1) was proposed by Altan and Aifantis (1992) who considered the special case, $c_1 = c_3 = c$, and $c_2 = 0$. Hence, with this simplification, Eq. (1) becomes

$$\sigma = \lambda(\text{tr } \epsilon)\mathbf{I} + 2G\epsilon - c\nabla^2[\lambda(\text{tr } \epsilon)\mathbf{I} + 2G\epsilon]. \quad (2)$$

Altan and Aifantis (1992) used Eq. (2), along with the equilibrium equation, $\text{div } \sigma = 0$, to solve the mode-III crack problem and found that the strain is finite at the crack tip. They also showed that for an atomic lattice, the gradient coefficient c can be estimated as $c = (0.25h)^2$, where h is the lattice constant. More generally, $2h$ is the characteristic length of the material cell for materials with unit cell (micro-medium), which may be interpreted as the periodic structure of a crystal lattice, a molecule of a polymer, a crystallite of a polycrystalline or a grain of a granular material (Mindlin, 1964). Internal characteristic length h is typically of the order of 10^{-8} m for some crystal lattices, and 10^{-4} m for some granular materials (Vardoulakis and Georgiadis, 1997). Hence, the value of c covers a large range for materials with different size of micro-medium. The determination of c by experiments is currently under way.

Constitutive Eq. (2) and equilibrium equation $\text{div } \sigma = 0$ can also be obtained from Casal's continuum (1972) in absence of surface energy, in which higher order stresses are the work conjugate of strain gradient variation. In this way, the boundary conditions are obtained by means of the variational method from Casal's continuum in the absence of double traction on the boundary surface $y = \text{constant}$ (Appendix A) as

$$\lambda\delta_{2j}\partial_2\epsilon_{1j} + 2G\partial_2\epsilon_{2j} = 0. \quad (3)$$

In the terms of the components of displacement field (u, v) for the plane strain problem, Eq. (3) yields

$$u_{,yy} + v_{,xy} = 0, \quad (4)$$

$$\lambda(u_{,xy} + v_{,yy}) + 2Gv_{,yy} = 0. \quad (5)$$

The extra boundary conditions (4) and (5) are different from those used in the simple strain gradient theory of elasticity (Altan and Aifantis, 1992; Ru and Aifantis, 1993) in which it is assumed that second partial derivative of displacement normal to the boundary is zero ($\frac{\partial^2 u}{\partial n^2} = 0$), or

$$u_{,yy} = 0, \quad (6)$$

$$v_{,yy} = 0 \quad (7)$$

for boundary $y = \text{constant}$. Although the boundary condition ($\frac{\partial^2 u}{\partial n^2} = 0$) has been used in the literature, the authors were not able to find any discussion explaining how they were obtained. Eqs. (6) and (7) imply that $v_{,xy}$ can be neglected with respect to $u_{,yy}$, and $u_{,xy}$ can be neglected with respect to $v_{,yy}$. Since these conditions

in general cannot be justified, the boundary conditions (4) and (5) are used in the solutions presented in this paper.

Ru and Aifantis (1993) later proposed a simple approach to solve boundary-value problems using the simple gradient theory of elasticity and established a simple relationship between the “gradient” displacement and the “classical” displacement for a traction-prescribed boundary-value problem as

$$(1 - c\nabla^2)\mathbf{u} = \mathbf{u}^0, \quad (8)$$

where \mathbf{u} is the displacement field considering gradient theory of elasticity, and \mathbf{u}^0 is the displacement field considering classical theory of elasticity.

One of the particular problems Ru and Aifantis (1993) solved using Eq. (8) with the boundary conditions (6) and (7) is the Flamant problem. By their approach, one extra boundary condition was needed to obtain a closed form solution for this problem. The solution obtained by them is complicated which makes it difficult to obtain a closed form solution for arbitrary line loading by superposition of the fundamental solution of the Flamant problem. In this paper, instead of superposition and boundary conditions (6) and (7), Fourier integral transforms with boundary condition (4) and (5) are used to obtain a general solution for a symmetrical line loading with prescribed normal tractions. The solution for the Flamant problem is then derived from the general solution as a special case without the need for any extra boundary conditions.

In what follows, a plane strain problem for a symmetrical line loading with prescribed normal tractions on a semi-infinite elastic solid is considered using gradient elasticity. The Navier equations of equilibrium of the plane strain problem are solved systematically using integral transformation techniques and general solutions for the plane strain problem are obtained using boundary conditions (4) and (5). The analytical solutions for the Flamant problem are derived from the general solutions to demonstrate how gradient elasticity can eliminate the singularity at the point of application of the load as predicted by classical elasticity. The analytical solutions obtained for constant normal tractions are also derived and compared with the classical solution. The solutions are used to demonstrate the influence of the gradient coefficient c on the deformation under constant normal traction and the size-dependency of the resulting deformation, i.e. the displacement normalized by length over which the load is applied becomes smaller with decreasing the length, a trend different from size-independency implied by classical elasticity.

2. Formulation for plane strain problem

The displacement field for the plane strain problem is assumed to be of the form

$$u = u(x, y), \quad v = v(x, y) \quad \text{and} \quad w \equiv 0. \quad (9)$$

The components of strain tensor corresponding to these displacements are

$$\varepsilon_x = \frac{\partial u}{\partial x}, \quad \varepsilon_y = \frac{\partial v}{\partial y}, \quad 2\gamma_{xy} = \frac{\partial u}{\partial y} + \frac{\partial v}{\partial x}, \quad \varepsilon_z = 0, \quad \gamma_{xz} = 0 \quad \text{and} \quad \gamma_{yz} = 0. \quad (10)$$

The constitutive Eq. (2) can be rewritten as

$$\sigma_{ij} = \lambda\varepsilon_{kk}\delta_{ij} + 2G\varepsilon_{ij} - c\{\lambda\varepsilon_{kk}\delta_{ij} + 2G\varepsilon_{ij}\}_{,mm} \quad (11)$$

and the components of the stress tensor are

$$\sigma_x = \lambda(\varepsilon_x + \varepsilon_y) + 2G\varepsilon_x - c\{\lambda(\varepsilon_x + \varepsilon_y) + 2G\varepsilon_x\}_{,mm}, \quad (12)$$

$$\sigma_y = \lambda(\varepsilon_x + \varepsilon_y) + 2G\varepsilon_y - c\{\lambda(\varepsilon_x + \varepsilon_y) + 2G\varepsilon_y\}_{,mm}, \quad (13)$$

$$\sigma_z = \lambda(\varepsilon_x + \varepsilon_y) - c\{\lambda(\varepsilon_x + \varepsilon_y)\}_{,mm}, \quad (14)$$

$$\tau_{xy} = 2G\epsilon_{xy} - 2Gc\{\epsilon_{xy}\}_{,mm} \quad (15)$$

and

$$\tau_{xz} = 0, \quad \tau_{yz} = 0.$$

Substitution of the stresses σ_{ij} into the equilibrium equations in the absence of body forces

$$\sigma_{ij,j} = 0 \quad (16)$$

yields

$$\begin{aligned} \lambda \left(\frac{\partial^2 u}{\partial x^2} + \frac{\partial^2 v}{\partial x \partial y} \right) + 2G \frac{\partial^2 u}{\partial x^2} - c \nabla^2 \left\{ \left(\frac{\partial^2 u}{\partial x^2} + \frac{\partial^2 v}{\partial x \partial y} \right) + 2G \frac{\partial^2 u}{\partial x^2} \right\} + G \left(\frac{\partial^2 u}{\partial y^2} + \frac{\partial^2 v}{\partial x \partial y} \right) \\ - cG \nabla^2 \left(\frac{\partial^2 u}{\partial y^2} + \frac{\partial^2 v}{\partial x \partial y} \right) = 0, \end{aligned} \quad (17)$$

$$\begin{aligned} \lambda \left(\frac{\partial^2 u}{\partial x \partial y} + \frac{\partial^2 v}{\partial y^2} \right) + 2G \frac{\partial^2 v}{\partial y^2} - c \nabla^2 \left\{ \lambda \left(\frac{\partial^2 u}{\partial x \partial y} + \frac{\partial^2 v}{\partial y^2} \right) + 2G \frac{\partial^2 v}{\partial y^2} \right\} + G \left(\frac{\partial^2 u}{\partial x \partial y} + \frac{\partial^2 v}{\partial x^2} \right) \\ - cG \nabla^2 \left(\frac{\partial^2 u}{\partial x \partial y} + \frac{\partial^2 v}{\partial x^2} \right) = 0. \end{aligned} \quad (18)$$

Taking Fourier transformation of Eqs. (17) and (18) and rearranging the results along with the relationship

$$\int_{-\infty}^{\infty} \nabla^2 f(x, y) e^{i\xi x} dx = \left(\frac{d^2}{dy^2} - \xi^2 \right) \int_{-\infty}^{\infty} f(x, y) e^{i\xi x} dx, \quad (19)$$

the following equations are obtained:

$$-G \left[c \frac{d^4 \bar{u}}{dy^4} - (1 + c\xi^2) \frac{d^2 \bar{u}}{dy^2} \right] + (\lambda + 2G) \xi^2 \left[c \frac{d^2 \bar{u}}{dy^2} - (1 + c\xi^2) \bar{u} \right] + \left\{ (\lambda + G) \xi \left[c \frac{d^3 \bar{v}}{dy^3} - (1 + c\xi^2) \frac{d \bar{v}}{dy} \right] \right\} i = 0, \quad (20)$$

$$-(\lambda + 2G) \left[c \frac{d^4 \bar{v}}{dy^4} - (1 + c\xi^2) \frac{d^2 \bar{v}}{dy^2} \right] + G \xi^2 \left[c \frac{d^2 \bar{v}}{dy^2} - (1 + c\xi^2) \bar{v} \right] + \left\{ (\lambda + G) \xi \left[c \frac{d^3 \bar{u}}{dy^3} - (1 + c\xi^2) \frac{d \bar{u}}{dy} \right] \right\} i = 0, \quad (21)$$

where

$$\bar{u}(\xi, y) = \int_{-\infty}^{\infty} u(x, y) e^{i\xi x} dx,$$

$$\bar{v}(\xi, y) = \int_{-\infty}^{\infty} v(x, y) e^{i\xi x} dx,$$

are the Fourier transforms of $u(x, y)$ and $v(x, y)$, with the inverse transforms

$$u(x, y) = \frac{1}{2\pi} \int_{-\infty}^{\infty} \bar{u}(\xi, y) e^{-i\xi x} d\xi,$$

$$v(x, y) = \frac{1}{2\pi} \int_{-\infty}^{\infty} \bar{v}(\xi, y) e^{-i\xi x} d\xi,$$

and $i = \sqrt{-1}$.

Letting

$$P = c \frac{d^2 \bar{u}}{dy^2} - (1 + c\xi^2) \bar{u} \quad (22)$$

and

$$Q = c \frac{d^2 \bar{v}}{dy^2} - (1 + c\xi^2) \bar{v}. \quad (23)$$

Eqs. (20) and (21) become

$$-G \frac{d^2 P}{dy^2} + (\lambda + 2G) \xi^2 P + (\lambda + G) \xi \frac{dQ}{dy} \mathbf{i} = 0 \quad (24)$$

and

$$-(\lambda + 2G) \frac{d^2 Q}{dy^2} + G \xi^2 Q + (\lambda + G) \xi \frac{dP}{dy} \mathbf{i} = 0. \quad (25)$$

From Eqs. (24) and (25), it follows that

$$\left(\frac{d^2}{dy^2} - \xi^2 \right) P = 0 \quad \text{and} \quad \left(\frac{d^2}{dy^2} - \xi^2 \right) Q = 0.$$

So

$$P = (a_1 + a_2 y) e^{|\xi|y} + (a_3 + a_4 y) e^{-|\xi|y} \quad (26)$$

and

$$Q = (a_5 + a_6 y) e^{|\xi|y} + (a_7 + a_8 y) e^{-|\xi|y}, \quad (27)$$

where a_1 – a_8 are constants.

The expressions of \bar{u} and \bar{v} can be derived from Eqs. (22), (23), (26) and (27), along with the condition that \bar{u} and \bar{v} both go to zero as y goes to infinity

$$\bar{u} = l_1 e^{-\sqrt{\frac{1}{c} + \xi^2} y} + (k_1 + k_2 y) e^{-|\xi|y} \quad (28)$$

and

$$\bar{v} = l_2 e^{-\sqrt{\frac{1}{c} + \xi^2} y} + (k_3 + k_4 y) e^{-|\xi|y}. \quad (29)$$

Here l_1 , l_2 , k_1 , k_2 , k_3 , k_4 are functions of ξ .

Taking Fourier transformation of Eqs. (12), (13), (15) and using Eqs. (28) and (29) yields the stress components in the transformed domain as

$$\bar{\sigma}_x = \lambda[(1 - 2c\xi^2 - |\xi|y)k_4 - k_3|\xi|]e^{-|\xi|y} - (\lambda + 2G)\xi[(2c|\xi| + y)k_2 + k_1]e^{-|\xi|y}\mathbf{i}, \quad (30)$$

$$\bar{\sigma}_y = (\lambda + 2G)[(1 - 2c\xi^2 - |\xi|y)k_4 - k_3|\xi|]e^{-|\xi|y} - \lambda\xi[(2c|\xi| + y)k_2 + k_1]e^{-|\xi|y}\mathbf{i} \quad (31)$$

and

$$\bar{\tau}_{xy} = G[(1 - 2c\xi^2 - |\xi|y)k_2 - k_1|\xi|]e^{-|\xi|y} - G\xi[(2c|\xi| + y)k_4 + k_3]e^{-|\xi|y}\mathbf{i}. \quad (32)$$

Also, when \bar{u} and \bar{v} , given in Eqs. (28) and (29), respectively, are substituted in Eqs. (20) and (21) the relationship between k_1 , k_2 , k_3 and k_4 are obtained as

$$k_2 = \text{Sign}(\xi)k_4i \quad (33)$$

and

$$\frac{\lambda + 3G}{\lambda + G}k_2 - \xi k_3i + \text{Sign}(\xi)k_1 = 0. \quad (34)$$

3. General solution for semi-infinite elastic solid subjected to a symmetrical line loading

In this section the deformation of a semi-infinite elastic solid body subjected to an external pressure at its bounding surface is considered. The elastic medium is bounded by a plane of infinite extent $y = 0$ as shown in Fig. 1. The y -axis is taken normal to the plane of the otherwise unbounded medium and points into the semi-infinite medium. It is assumed that this domain is under the action of a surface pressure p applied along the x -axis, which varies along the surface.

For simplicity, $p(x)$ is taken as an even function of x which results in symmetrical deformations, i.e.,

$$u(-x, y) = -u(x, y) \quad (35)$$

and

$$v(-x, y) = v(x, y). \quad (36)$$

The symmetrical deformation field then in turn leads to

$$k_1(-\xi) = -k_1(\xi), \quad k_2(-\xi) = -k_2(\xi), \quad l_1(-\xi) = -l_1(\xi),$$

$$k_3(-\xi) = k_3(\xi), \quad k_4(-\xi) = k_4(\xi), \quad l_2(-\xi) = l_2(\xi)$$

and

$$u = \frac{-i}{\pi} \int_0^\infty \bar{u}(\xi, y) \sin(\xi x) d\xi, \quad (37)$$

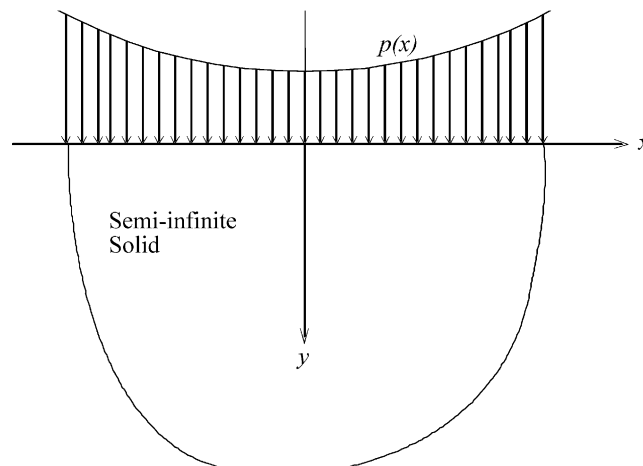


Fig. 1. Semi-infinite elastic solid subjected to an even surface pressure $p(x)$.

$$v = \frac{1}{\pi} \int_0^\infty \bar{v}(\xi, y) \cos(\xi x) d\xi. \quad (38)$$

The relevant traction boundary conditions are adopted as

$$\sigma_y = -p(x), \quad (39)$$

$$\tau_{xy} = 0, \quad (40)$$

at $y = 0$.

Eq. (40) results in

$$(1 - 2c\xi^2)k_2 - \xi k_1 - \xi(2\xi c k_4 + k_3)i = 0. \quad (41)$$

Hence, the coefficients k_1, k_2, k_3 are solved in terms of k_4 using Eqs. (33), (34), and (41) for $\xi \geq 0$

$$k_1 = -\left(2c\xi^2 + \frac{G}{\lambda + G}\right) \frac{i}{\xi} k_4, \quad (42)$$

$$k_2 = k_4 i, \quad (43)$$

$$k_3 = \left(-2c\xi^2 + \frac{\lambda + 2G}{\lambda + G}\right) \frac{1}{\xi} k_4. \quad (44)$$

Subsequently, the boundary condition (39) together with the expressions for k_1, k_2, k_3 in terms of k_4 and Eq. (31), yields the stress components σ_y at $y = 0$ as

$$\sigma_y = \frac{1}{\pi} \int_0^\infty \bar{\sigma}_y \cos(\xi x) d\xi = -\frac{2G}{\pi} \int_0^\infty k_4(\xi) \cos(\xi x) d\xi. \quad (45)$$

Hence

$$\int_0^\infty k_4(\xi) \cos(\xi x) d\xi = \frac{\pi p(x)}{2G} \quad (46)$$

and the expression for k_4 can be obtained as

$$k_4(\xi) = \frac{1}{G} \int_0^\infty p(x) \cos(\xi x) dx. \quad (47)$$

To solve for the constants l_1 and l_2 , the extra gradient boundary conditions (4) and (5) are required as a result of the higher gradient terms utilized.

Eqs. (4) and (5), together with Eqs. (28), (29) and (37), (38), yield

$$i\left(\frac{1}{c} + \xi^2\right)l_1 - \xi\sqrt{\frac{1}{c} + \xi^2}l_2 + i\xi^2k_1 - 2i\xi k_2 - \xi^2k_3 + \xi k_4 = 0 \quad (48)$$

and

$$i\lambda\sqrt{\frac{1}{c} + \xi^2}l_1 + (\lambda + 2G)\left(\frac{1}{c} + \xi^2\right)l_2 + i\lambda\xi^2k_1 - i\lambda\xi k_2 + (\lambda + 2G)\xi^2k_3 - 2(\lambda + 2G)\xi k_4 = 0, \quad (49)$$

which implies

$$l_1(\xi) = \text{ic} \left[\frac{2(\lambda + 2G)\xi}{\lambda} \frac{\lambda(1 + 2c\xi^2) + 2cG\xi\sqrt{\frac{1}{c} + \xi^2}}{\lambda + 2G + 2c(\lambda + G)\xi^2} - \frac{4G\xi^2}{\lambda\sqrt{\frac{1}{c} + \xi^2}} \right] k_4 \quad (50)$$

and

$$l_2(\xi) = \frac{2c\xi^2 \left[\lambda(1 + 2c\xi^2) + 2cG\xi\sqrt{\frac{1}{c} + \xi^2} \right]}{[\lambda + 2G + 2c(\lambda + G)\xi^2]\sqrt{\frac{1}{c} + \xi^2}} k_4. \quad (51)$$

Substitution of Eqs. (42)–(44) into Eqs. (30)–(32) for $\xi \geq 0$ and taking inverse Fourier transforms yields the stress components as

$$\sigma_x = -\frac{2G}{\pi} \int_0^\infty k_4(1 - \xi y) e^{-\xi y} \cos(\xi x) d\xi, \quad (52)$$

$$\sigma_y = -\frac{2G}{\pi} \int_0^\infty k_4(1 + \xi y) e^{-\xi y} \cos(\xi x) d\xi, \quad (53)$$

$$\tau_{xy} = -\frac{2Gy}{\pi} \int_0^\infty \xi k_4 e^{-\xi y} \sin(\xi x) d\xi, \quad (54)$$

which show that stress distribution is only dependent on k_4 , and k_4 is not related with the extra gradient boundary conditions. From Eq. (47) it can be seen that k_4 is a function of the loading $p(x)$. Hence, the stress distribution obtained here remains the same as the one in classical elasticity. Ru and Aifantis (1993) have shown that the stress distribution obtained with the boundary conditions (6) and (7) was identical with the one in classical elasticity also. However, the displacement field dependent which is dependent on l_1 and l_2 will differ for the two sets of boundary conditions.

Particularly, the surface displacement u and v may be derived by substituting Eqs. (42)–(44) and (50), (51) into Eqs. (28) and (29), and using Eqs. (37) and (38) at $y = 0$:

$$u(x, 0) = -\frac{i}{\pi} \int_0^\infty \left[l_1(\xi) - 2ic\xi k_4(\xi) - i\frac{G}{\lambda + G} \frac{1}{\xi} k_4(\xi) \right] \sin(\xi x) d\xi \quad (55)$$

and

$$v(x, 0) = \frac{1}{\pi} \int_0^\infty \left[l_2(\xi) - 2c\xi k_4(\xi) + \frac{\lambda + 2G}{\lambda + G} \frac{1}{\xi} k_4(\xi) \right] \cos(\xi x) d\xi. \quad (56)$$

It can be shown that the surface displacements represented by Eqs. (55) and (56) reduce to the classical solution at $c = 0$. Once k_4 is obtained, the surface displacements due to arbitrary symmetrical line loading with prescribed normal traction can be obtained from Eqs. (55) and (56). The solution for three typical surface pressure distributions are shown in the following.

4. Solutions for special surface pressure distributions

As special cases to the above general solution, the problem with a typical Hertzian pressure distribution in classical elasticity for $|x| \leq a$, the Flamant problem and constant pressure for $|x| \leq a$ will be discussed (see Fig. 2).

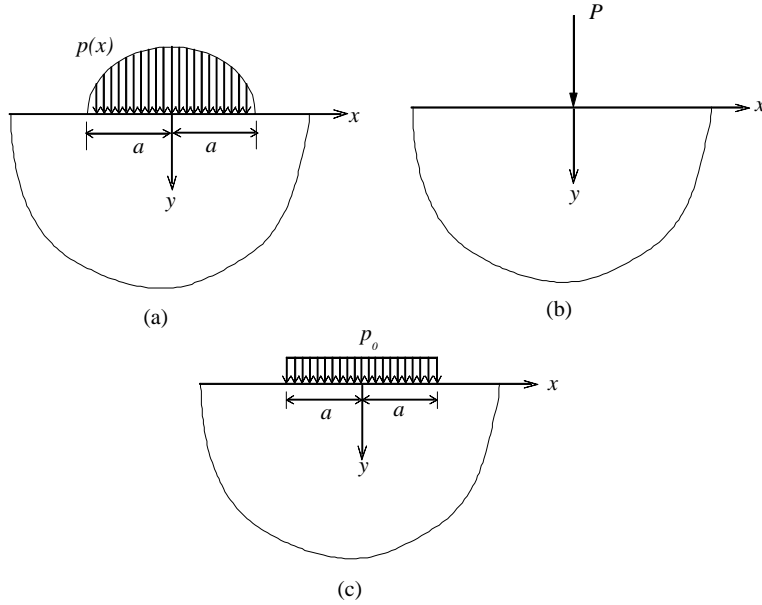


Fig. 2. Special surface pressure distribution: (a) a typical Hertzian pressure distribution; (b) concentrated force; (c) constant surface pressure.

4.1. A Hertzian pressure distribution for $|x| \leq a$ from classical elasticity

A typical Hertzian pressure distribution $p(x)$ (Johnson, 1985) on the surface in classical elasticity is defined by the relation

$$\begin{cases} p(x) = p_0 \left(1 - \frac{x^2}{a^2}\right)^{1/2} & |x| \leq a, \\ p(x) = 0 & |x| > a. \end{cases}$$

Substituting this pressure distribution into Eq. (47), k_4 is solved as

$$k_4(\xi) = \frac{\pi p_0 J_1(a\xi)}{2G\xi}. \quad (57)$$

The surface displacements are determined by substituting k_4 from Eq. (57) into Eqs. (50), (51) and Eqs. (55), (56).

4.2. Flamant problem

For the Flamant problem, a point force of magnitude p acts at the origin of the coordinate system on the boundary surface. For this case, k_4 can be calculated from Eq. (47) by assuming p acting over a length of $2a$ ($|x| < a$) and then letting $a \rightarrow 0$, i.e.

$$k_4(\xi) = \lim_{a \rightarrow 0} \frac{1}{G} \int_0^a \frac{p}{2a} \cos(\xi x) dx = \frac{p}{2G}.$$

The components of the surface displacement are obtained by substituting the expression k_4 into Eqs. (50), (51) and Eqs. (55), (56). Due to their complicated form, the expressions for surface displacements are not given here. It is shown that the surface displacement in y direction be finite at the origin $(0, 0)$ in Section 5.

It should be noted that the gradient elasticity solution reduces to the classical elasticity solution (Johnson, 1985) by letting $c = 0$ in Eqs. (55) and (56), considering $\frac{\lambda+2G}{G(\lambda+G)} = \frac{4(1-v^2)}{E}$, $\frac{1}{\lambda+G} = \frac{2(1+v)(1-2v)}{E}$.

$$u(x, 0) = \frac{-(1-2v)(1+v)p}{2E}, \quad (58)$$

$$v(x, 0) = \frac{2(1-v^2)}{\pi E} p \log x + C_0. \quad (59)$$

Hence, the gradient elasticity solution to the Flamant problem is obtained relatively easily using the integral transformation techniques, and the singularity at the origin predicted by the classical elasticity solution disappears.

4.3. Constant surface pressure for $|x| \leq a$

$$p(x) = p_0 \quad |x| \leq a.$$

In like fashion,

$$k_4(\xi) = \frac{p_0 \sin(a\xi)}{G\xi}. \quad (60)$$

The surface displacements obtained by substituting the expression k_4 into Eqs. (50), (51) and Eqs. (55), (56) are evaluated by using MATHEMATICA in Section 5.

The gradient elasticity solution reduces to the classical elasticity solution (Johnson, 1985) by letting $c = 0$ in Eqs. (55), (56).

$$u(x, 0) = \begin{cases} \frac{-p_0(1+v)(1-2v)}{E} x, & |x| \leq a, \\ \frac{-p_0(1+v)(1-2v)}{E} a, & x > a, \\ \frac{p_0(1+v)(1-2v)}{E} a, & x < -a. \end{cases}$$

and

$$v(x, 0) = \frac{-p_0(1-v^2)}{\pi E} \left[(x+a) \log \left(\frac{x+a}{a} \right)^2 - (x-a) \log \left(\frac{x-a}{a} \right)^2 \right] + C.$$

5. The results

The surface displacement in y direction due to the typical Hertzian pressure distribution ($p_0 = 150$ G N/m, loading length $2a = 1.0$ μm) and classical one are plotted in Fig. 3 for an elastic solid with $E = 135$ GPa, $v = 0.3$, $c = 0.05$ μm^2 . The value of c chosen is in the range of given for some materials in the paper (Vardoulakis and Georgiadis, 1997). The x distance and the displacement are normalized by a . It is shown in Fig. 3 that the normalized deformed depth at origin in gradient elasticity is smaller than the one in classical elasticity.

To illustrate the gradient theory can eliminate the undesirable singularity for the Flamant problem, the solutions in the y direction for the Flamant problem and classical one are plotted in Fig. 4 for the same elastic solid as in Fig. 3. It is assumed that the displacement in the y direction on the surface is zero at a distance $x_0 = 1.0$ μm . The x distance and the displacement are normalized by x_0 and $\frac{2(1-v^2)}{\pi E} p$, i.e. the $\eta = \frac{x}{x_0}$, the normalized displacement in y direction $V(\eta, 0) = \frac{\pi E}{2(1-v^2)} v(x, 0)$. Fig. 4 shows that the displacement at the origin is finite, and also $\frac{dv(0,0)}{dx} = 0$, i.e. the symmetry of displacement with respect to x -axis is naturally

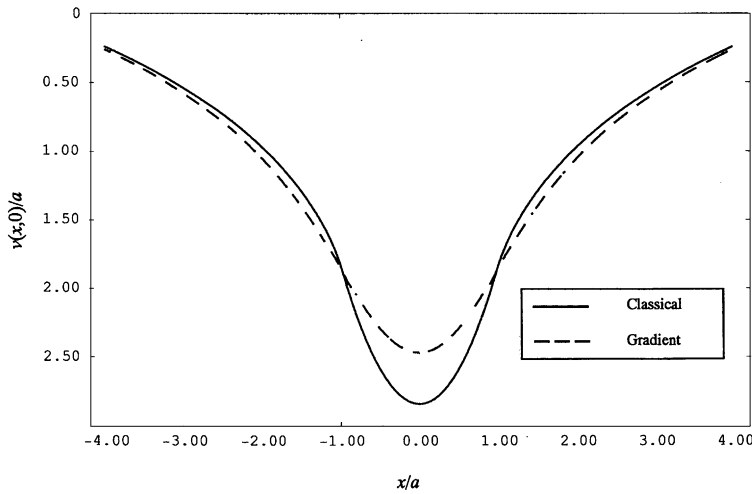


Fig. 3. Comparison of the surface displacement between gradient solution and the classical solution for Hertzian pressure distribution with loading length $2a = 1 \mu\text{m}$.

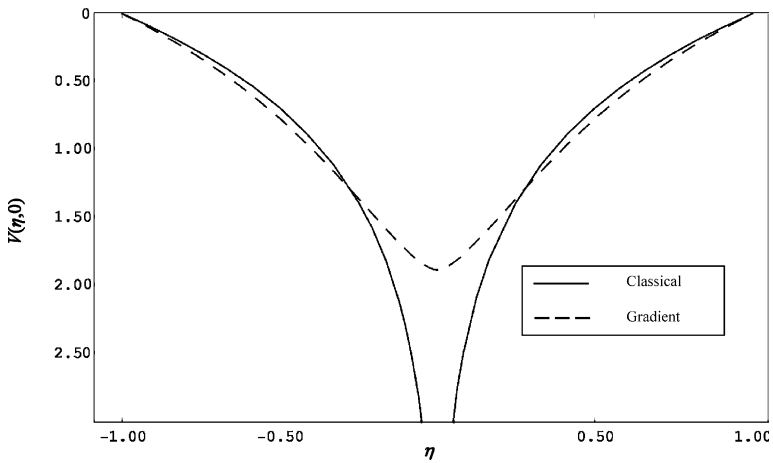


Fig. 4. Comparison of the surface displacement between gradient solution and the classical solution for Flamant problem.

satisfied. Ru and Aifantis (1993) had to use this symmetry as an extra boundary condition to achieve the solution, through their simple approach with the boundary condition (6) and (7).

The deformed surface profiles in Fig. 5(a) are plotted by using the classical solutions for the same elastic solid subjected to the same constant pressure ($p_0 = 150 \text{ G N/m}$) applied over a length of $2a$ where a is varied from 0.2 to 1.0 μm . After being normalized by half pressure loading length a , the plots of the depth $v(x, 0)/a$ vs. position x/a all lie on the same curve irrespective of the length $2a$ as shown in Fig. 5(b). Classical elasticity, by its scale-free nature, cannot predict the size-dependency of the resulting deformation.

In gradient elasticity, the solution obtained is used to demonstrate size-dependency of the resulting deformation. The deformed surface profiles in Fig. 6 are plotted by using the analytical solutions for the same elastic solid as in Fig. 3 subjected to the same pressure applied over the length of $2a$. The curves in

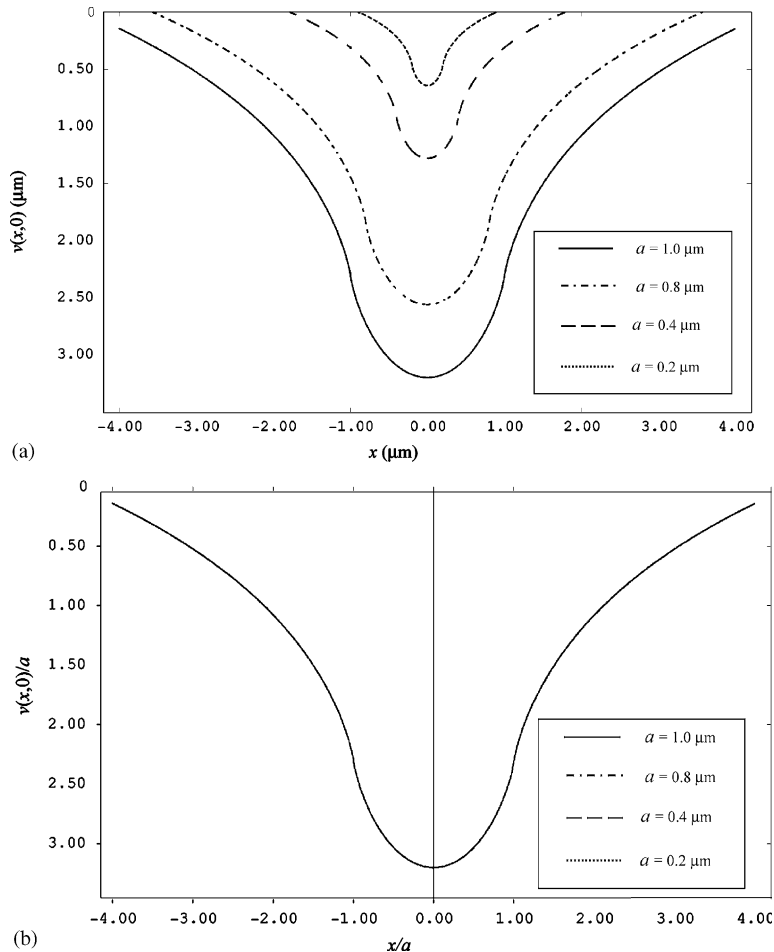


Fig. 5. (a) The deformed surface profiles for several loading length $2a$ as predicted by classical elasticity. (b) Normalized deformed surface profiles due to constant pressure for several loading lengths $2a$ as predicted by classical elasticity.

Fig. 6 were generated with a constant gradient coefficient $c = 0.05 \mu\text{m}^2$ for different pressure loading lengths $2a$. In this figure, the surface displacements $v(x, 0)$ and the position x have been normalized by half pressure loading length a , and it is observed that the normalized curves $v(x, 0)/a$ for different a do not coincide as it is the case for the classical solution. The solid line on the same figure depicts the classical solution. It shows that a decrease in the loading length causes a decrease in the normalized deformed depth. The curves converge to the solid line representing the classical solution as the length increases in Fig. 6. So, when the length associated with the deformation field is large, the influence of strain gradients on the deformation is small and classical elasticity theory suffices. It is also justified that effect of strain gradient becomes important when indentation tests are on small-scale such as micro-indentation test or nano-indentation tests at the sub-micron scale (Fleck and Hutchinson, 1997). The result due to the effect of strain gradients in elasticity is interestingly consistent with size effect in plasticity that hardness increases with decreasing indent size (Shu and Fleck, 1998; Matthew and Hutchinson, 1998). The effect of the magnitude of gradient coefficients c on deformation is illustrated in Fig. 7. Here, the same elastic solid as in Fig. 6 is used with loading length $2a$ being $1.0 \mu\text{m}$. The curves were generated for different gradient coefficient c , with the solid line representing the classical solution. It is observed that materials with larger gradient coefficient c have

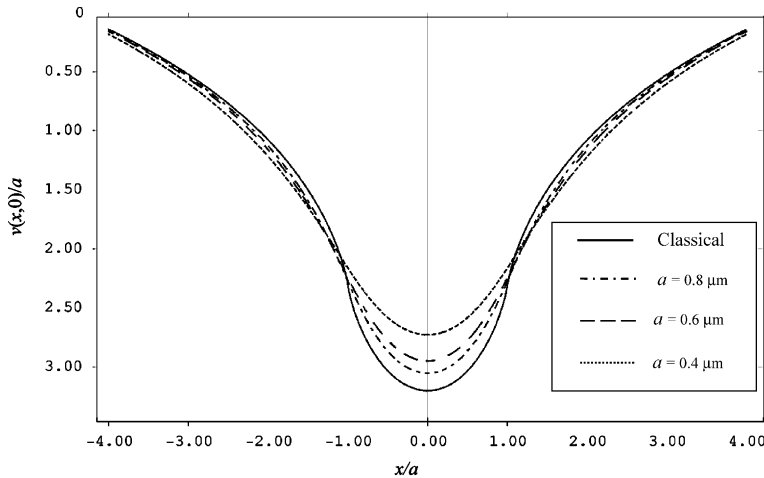


Fig. 6. Normalized deformed surface profiles due to constant pressure for several loading lengths $2a$ and gradient coefficient $c = 0.05 \mu\text{m}^2$.

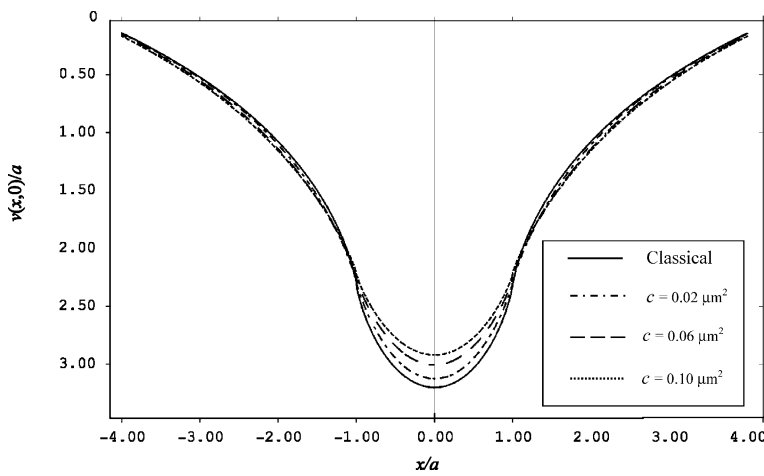


Fig. 7. Deformed surface profiles for several gradient elasticity coefficient c , for loading length $2a = 1.0 \mu\text{m}$.

smaller deformed depth. It also can be shown that the influence of gradient coefficient c on the deformation is more pronounced as the loading length decreases.

From the above three figures, the analytical solution within the gradient elasticity for elastic solids due to a constant contact pressure appears to be an excellent means to show the effect of strain gradient in the deformation of elastic solid. It shows that loading size at small scales play an important role in the deformation of elastic materials due to incorporating the gradient coefficient c in the constitutive law.

6. Conclusions

A simple gradient theory of elasticity with an additional material parameter (gradient coefficient c) is used to obtain a general solution for a two-dimensional solid subjected to a symmetrical line loading with

prescribed normal tractions $p(x)$. Integral transformation technique is used in the solution and higher order conditions are utilized. To gain insight on the influence of loading size on the deformation of elastic materials as inferred by the gradient coefficient c , the analytical solution for semi-infinite elastic solid subjected to a constant surface pressure is investigated for different loading lengths and gradient coefficient c . It is shown the effect of strain gradient in elasticity becomes significant for the kind of line loading problem at small scales, when compared with classical elasticity.

Acknowledgements

The authors gratefully acknowledge the support of College of Engineering at Michigan Technological University during the course of the study.

Appendix A

The strain-energy density in Casal's continuum (Casal, 1972) with respect to a Cartesian coordinate system expressed as

$$W = \frac{1}{2} \lambda \varepsilon_{ii} \varepsilon_{jj} + G \varepsilon_{ij} \varepsilon_{ji} + l^2 \left(\frac{1}{2} \lambda \partial_k \varepsilon_{ii} \partial_k \varepsilon_{jj} + G \partial_k \varepsilon_{ij} \partial_k \varepsilon_{ji} \right) + l' v_k \partial_k \left(\frac{1}{2} \lambda \varepsilon_{ii} \varepsilon_{jj} + G \varepsilon_{ij} \varepsilon_{ji} \right), \quad (\text{A.1})$$

where l , l' are characteristic material lengths, and v_k , $\partial_k v_k = 0$, is a director field equal to the unit outer normal n_k on the boundaries. It can be shown that after integrating W over the domain and applying the Stokes theorem, the last term in Eq. (A.1) takes the form

$$l' \left(G \int_{\partial\Omega} \varepsilon_{ij} \varepsilon_{ij} dA + \frac{1}{2} \lambda \int_{\partial\Omega} \varepsilon_{ii} \varepsilon_{jj} dA \right),$$

which can be interpreted as surface energy. Total strain energy given in Eq. (A.1) is positive-definite for $3\lambda + 2G > 0$, $G > 0$, and l , $l' \geq 0$. In the strain-energy Eq. (A.1) from Casal's continuum (Casal, 1972), the Cauchy stresses τ_{ij} , the couple stresses μ_{kij} and the total stresses σ_{ij} with respect to a Cartesian system are defined as

$$\tau_{ij} = \partial W / \partial \varepsilon_{ij} = \lambda \delta_{ij} \varepsilon_{kk} + 2G \varepsilon_{ij} + l' (\lambda \delta_{ij} v_k \partial_k \varepsilon_{ll} + 2G v_k \partial_k \varepsilon_{ij}), \quad (\text{A.2})$$

$$\mu_{kij} = \partial W / \partial \varepsilon_{ij,k} = l^2 (\lambda \delta_{ij} \partial_k \varepsilon_{ll} + 2G \partial_k \varepsilon_{ij}) + l' (\lambda \delta_{ij} v_k \varepsilon_{ll} + 2G v_k \varepsilon_{ij}), \quad (\text{A.3})$$

$$\sigma_{ij} = \tau_{ij} - \partial_k \mu_{kij} = \lambda \delta_{ij} \varepsilon_{kk} + 2G \varepsilon_{ij} - l^2 \nabla^2 (\lambda \delta_{ij} \varepsilon_{ll} + 2G \varepsilon_{ij}). \quad (\text{A.4})$$

From strain energy (A.1), the variation of the total potential energy in a volume Ω , which is bounded by the smooth surface $\partial\Omega$, is obtained by using the divergence theorem and the surface divergence theorem:

$$\delta \int_{\Omega} W dV = - \int_{\Omega} \partial_i \sigma_{ij} \delta u_j dV + \int_{\partial\Omega} \{ [n_i \sigma_{ij} - D'_i (n_k \mu_{kij}) + (D'_i n_l) n_k n_i \mu_{kij}] \delta u_j + n_k n_i \mu_{kij} (n_m \partial_m u_j) \} dA, \quad (\text{A.5})$$

D'_i stands for the derivatives in the tangential direction to the boundaries.

Based on the principle of virtual work, it is assumed that the potential energy has the form

$$\delta \int_{\Omega} W = \int_{\Omega} F_j \delta u_j dV - \int_{\partial\Omega} [T_j \delta u_j + Q_j (\partial_i u_j n_i)] dA, \quad (\text{A.6})$$

where F_j is the external body force, T_j and Q_j are traction and double traction on the boundary, respectively. From Eqs. (A.5) and (A.6), it follows that the equation of equilibrium is

$$\partial_i \sigma_{ij} + F_j = 0 \quad (\text{A.7})$$

and the boundary conditions are

$$u_j = \bar{u}_j \quad \text{or} \quad n_i \sigma_{ij} - D_i^l (n_k \mu_{kij}) + (D_l^l n_l) n_k n_i \mu_{kij} + T_j = 0, \quad (\text{A.8})$$

$$n_j \partial_j u_i = \bar{E}_i \quad \text{or} \quad n_k n_i \mu_{kij} + Q_j = 0, \quad (\text{A.9})$$

where \bar{u}_j and \bar{E}_i are prescribed on the appropriate portion of the boundary.

It is noted that the constitutive equations and equilibrium equations in a simple gradient theory of elasticity introduced by Aifantis and co-workers (Aifantis, 1992; Altan and Aifantis, 1992) reads

$$\boldsymbol{\sigma} = \lambda(\text{tr } \boldsymbol{\varepsilon}) \mathbf{I} + 2G\boldsymbol{\varepsilon} - c\nabla^2[\lambda(\text{tr } \boldsymbol{\varepsilon}) \mathbf{I} + 2G\boldsymbol{\varepsilon}], \quad (\text{A.10})$$

$$\text{div } \boldsymbol{\sigma} = 0. \quad (\text{A.11})$$

It is apparent that the constitutive Eq. (A.4) and equilibrium Eq. (A.7) in Casal's continuum theory with $c = l^2$ and $l' = 0$ are the same as those in the simple gradient theory of elasticity given in Eqs. (A.10) and (A.11) in a Cartesian coordinate system. Hence Casal's continuum theory can be used to derive the boundary conditions for a boundary value problem in the simple gradient theory of elasticity in a rigorous way.

The desired boundary conditions are obtained from Eqs. (A.9) and (A.11). For simplicity, it is assumed that there are no double tractions on the boundaries, i.e.,

$$n_k n_i \mu_{kij} = 0 \quad (\text{A.12})$$

or

$$c(\lambda \delta_{ij} \partial_k \varepsilon_{kl} + 2G \partial_k \varepsilon_{ij}) n_k n_i = 0. \quad (\text{A.13})$$

The extra boundary condition (A.13) may be used together with either displacement boundary conditions or traction boundary conditions. Altan and Aifantis (1997) showed that there exists uniqueness of solution for equilibrium Eq. (A.11) with the extra boundary condition (A.13) and displacement boundary conditions. For the traction boundary conditions, it should be noted that, in Eq. (A.8), $-D_i^l (n_k \mu_{kij}) + (D_l^l n_l) n_k n_i \mu_{kij}$ is not necessarily equal to zero. Therefore the classical form of traction boundary condition ($n_i \sigma_{ij} + T_j = 0$) is no longer the natural boundary condition in the present case though it has been used as one of the physically acceptable boundary conditions in the simple gradient theory of elasticity.

References

Aifantis, E.C., 1996. High order gradients and size effects. In: Carpinteri, A. (Ed.), *Size-Scale Effects in the Failure Mechanisms of Materials and Structures*. E & FN Spon, London, pp. 231–242.

Aifantis, E.C., 1992. On the role of gradients in the localization of deformation and fracture. *Int. J. Engng. Sci.* 30, 1279–1299.

Altan, B.S., Aifantis, E.C., 1992. On the structure of the mode-III crack-tip in gradient elasticity. *Scripta Met.* 26, 319–324.

Altan, B.S., Aifantis, E.C., 1997. On some aspects in the special theory of gradient elasticity. *J. Mech. Behavior Mater.* 8 (3), 231–282.

Casal, P., 1972. La theorie du second gradient et la capillarite. *C.R. Acad. Sci. Paris Ser. A* 274, 1571–1574.

Fleck, N.A., Hutchinson, J.W., 1997. Strain gradient plasticity. In: Hutchinson, J.W., Wu, T.Y. (Eds.), *Advances in Applied Mechanics*, vol. 33. Academic Press, New York, pp. 295–361.

Georgiadis, H.G., Vardoulakis, I., 1998. Anti-plane shear Lamb's problem treated by gradient elasticity with surface energy. *Wave Motion* 28, 353–366.

Gutkin, M.Yu., 2000. Nanoscopics of dislocations and disclinations in gradient elasticity. *Rev. Adv. Mater. Sci.* 1, 27–60.

Johnson, K.L., 1985. Contact Mechanics. Cambridge University Press, Cambridge.

Koiter, W.T., 1964. Couple stresses in the theory of elasticity, I and II. *Proceedings Koninklijke Nederlandse Akademie van Wetenschappen (B)* 67, 17–44.

Matthew, R.B., Hutchinson, J.W., 1998. The mechanics of size-dependent indentation. *J. Mech. Phys. Solids* 46 (10), 2049–2068.

Mindlin, R.D., 1964. Micro-structure in linear elasticity. *Arch. Rational Mech. Anal.* 16, 51–78.

Mindlin, R.D., 1965. Second gradient of strain and surface-tension in linear elasticity. *Int. J. Solids Struct.* 1, 417–438.

Ru, C.Q., Aifantis, E.C., 1993. A simple approach to solve boundary-value problems in gradient elasticity. *Acta Mech.* 101, 59–68.

Shu, J.Y., Fleck, N.A., 1998. The prediction of a size effect in micro-indentation. *Int. J. Solids Struct.* 35 (13), 1363–1383.

Toupin, R.A., 1962. Elastic materials with couple stresses. *Arch. Ration. Mech. Anal.* 11, 385–414.

Vardoulakis, I., Georgiadis, H.G., 1997. Sh surface waves in a homogeneous gradient-elastic half-space with surface energy. *J. Elast.* 47, 147–165.

Zhang, L., Huang, Y., Chen, J.Y., Hwang, K.C., 1998. The mode III full-field solution in elastic materials with strain gradient effects. *Int. J. Fract.* 92, 325–348.